Effect of Atmospheric Pressure Plasma Treatment and Surface Roughness on Osteoblastic Response and Osteoconductivity of Zirconia

2013

Shin Hye Chung, DDS, MSD

Department of Conservative Dentistry, Graduate School, Seoul National University
*(Directed by Prof., **Won-Jun Shon**, DDS, PhD)*

CONTENTS

ABSTRACT

Objective. The aim of this study was to evaluate osteoblast-like cell response and bone formation associated with implantation of roughened yttria-stabilized tetragonal zirconia polycrystal (Y-TZP) after an atmospheric pressure plasma (APP) treatment.

Materials and Methods. Disc-shaped specimens (Ø 13 × 1 mm) were prepared and divided into 4 groups depending on surface roughness and APP treatment. The disc-shaped surfaces were roughened by sandblasting followed by hydrofluoric (HF) acid etching. Surfaces were analyzed by XPS with contact angle measurement. Surface characteristics of disc samples were evaluated by SEM, CLSM and XPS analyses. The spreading of MG63 cells on the disc surfaces was observed by SEM after a 30-minute incubation period.

Screw-type dental implant fixture-shaped specimens with external hex (Ø 4 × 7 mm) were prepared and divided into four groups depending on surface roughness and APP treatment. The rough fixture-shaped specimens were manufactured in a net-shaped mold with a rugged surface by the powder injection technique. Osteoconductivity tests with various surface properties were performed in the mesial region of rabbit tibiae at 4 weeks following installation. Removal torque test (RTQ) and histomorphometric analyses were performed, and data were analyzed using 2-way ANOVA (p= 0.05).

Results. APP treatment enhanced the surface hydrophilicity of Y-TZP disc- and fixture-shaped specimens without topographical changes. The spreading of MG63 cells on plasma-treated disc surfaces at 30 minutes were higher compared to untreated surfaces (p<0.001), and the APP-treated fixture-shaped specimens exhibited significantly higher BIC values than those of untreated ones (p<0.001).

Conclusion. Atmospheric pressure plasma treatments increased surface hydrophilicity of Y-TZP and enhanced the initial spread of MG63 cells as well as osseointegration in rabbits.

Keywords: Zirconia; Atmospheric pressure plasma; Roughness; Osseointegration; Hydrophilicity

Student Number: 2011-30673

1. INTRODUCTION

Due to its biocompatibility and high long-term success rates, titanium (Ti) and its alloys have been widely used in joint replacement and dental implants.[1, 2] This well-documented material of choice can be altered to meet demands and overcome problems such as its metallic color and the potential for immunologic reactions.[3, 4] In dental implants, yttria-stabilized tetragonal zirconia polycrystal (Y-TZP), with its high mechanical and biological properties, is considered a viable alternative for titanium. The potential for osseointegration and successful clinical outcomes, as well as the associated esthetic properties were documented for Y-TZP implants.[5, 6]

Since osseointegration of dental implants occurs directly on the surface of the implanted materials, properties of these surfaces affect new bone formation.[7-9] Surface modifications of titanium implant materials have been performed to promote biocompatibility, enhancing cellular responses and integration with surrounding tissues. Studies regarding titanium implant surface modifications have revealed that modified surfaces accelerate biologic responses, leading to faster healing and earlier loading.[10, 11]

Studies related to Y-TZP surface roughness on bone apposition are limited, and those that have been published are controversial.[12, 13] A novel roughening

surface technique known as powder injection molding (PIM) was introduced for Y-TZP dental implants and showed promising results in an *in vivo* rabbit experiment.[14] PIM usually involves compounding ceramic powder with a blend of polymers or wax in a solvent.[15] Prior to sintering, the organic binders embedded in the molded parts are removed. Through this method, the surface roughness of Y-TZP implants was increased to the level defined as 'moderately rough' in commercially available Ti implants.[16]

Among the surface properties of dental implants, hydrophilicity is gaining interest.[17] Efforts to increase surface hydrophilicity have been made in the form of physicochemical modifications, and results in animal studies and in a recent human study have shown that osseointegration in the early healing phase is superior for hydrophilic surface implants compared to hydrophobic surface implants.[18-20] One popular method to improve surface hydrophilicity is to use gas plasma.[21] Non-thermal atmospheric pressure plasmas (APPs) used in biomedical applications have been shown to change the energy and chemistry of surfaces leading to increased surface reactivity.[22]

In this study, a chair-side pencil-type APP was applied to the roughened Y-TZP disc surface to evaluate the spread of MG63 cells *in vitro*. *In vivo* performance APPs and surface roughness of Y-TZP implants were examined in rabbits.

2. MATERIALS and METHODS

2.1. Cell Spread on APP-treated and Etched Y-TZP Surfaces

2.1.1. Preparation of disc specimens

Disc-shaped Y-TZP specimens (Table 1) 13 mm in diameter and 1 mm in thickness were prepared and divided into four groups (n=8) (Fig. 2a):

Group A: Control.

Group B: A roughened surface with sandblasting and HF etching.

Group C: An APP-treated Y-TZP disc specimen.

Group D: APP-treated after sandblasting and HF etching.

In Groups B and D, alumina (Al_2O_3) blasting followed by HF etching was performed to provide surface roughness. Alumina particles of 50 ㎛ were blasted at 0.2 MPa for 60 seconds. Specimens were fixed at a distance of 10 mm from the tip of the sandblaster, and the angle of particle delivery was 90 degrees. The tip was continuously moved in a circular direction during blasting. Following blasting, the surface was etched with 40% hydrofluoric (HF) acid for 10 minutes at a room temperature.

2.1.2. Non-thermal Atmospheric Pressure Plasma (APP) Treatment

A chair-side, pencil-type atmospheric pressure glow discharge plasma designed by Cho et al. (2011) was modified for surface treatment.[23] Helium

(He) was delivered into the tube at a flow rate of 2 L/min as a carrier gas with vaporized distilled water (DW) only, instead of the monomers that were used in the previous study.[23] A radiofrequency voltage of 1.9 kV and an output current of 2.9 mA were applied at 15 kHz. The flow rate of the vaporized water was controlled at a rate of 80 standard cubic centimeters per minute (sccm) using a mass flow controller (FC7700C, Aera Japan, Hachoiji, Japan). Treatment time was set at 60 seconds at a distance of 5 mm (Figure 1).

2.1.3. Surface characterizations

The surface of each groups was characterized by scanning electron microscopy (SEM, S-4700, Hitachi, Tokyo, Japan), confocal three-dimensional laser scanning microscopy (CLSM, 3D LSM, LSM 5 Pascal, Carl Zeiss, Jena, Germany), and atomic force microscopy (AFM, SPA-400, Seiko instruments, Chiba, Japan).

The average surface roughness (S_a) of the specimens was obtained by CLSM. A HeNe (Green, 543 nm) laser was used, and surface roughness was examined at 200× magnification. The measured area was 450 × 450 μm^2, and the average surface roughness was calculated using 6 randomly-selected points.

Detailed surface microstructures were observed by AFM. Images of 256 ×

256 pixels were obtained with a scan size of 10 × 10 μm^2 at a scanning rate of 0.1Hz.

Surface hydrophilicity was examined with a contact angle analyzer (Phoenix 150, Surface ElectroOptics, Seoul, Korea) using the Sessile drop technique. To evaluate the performance of vaporized DW in the plasma treatment, additional experiments were performed measuring contact angles after plasma treatment without DW for Groups A and B. Measurements were determined using distilled water at room temperature. Five samples were tested, and the values were averaged.

Surface chemical composition was evaluated by X-ray photoelectron spectroscopy (XPS, Sigma Probe, Thermo VG, Thermo Fisher Scientific, Hemel, Hempstead, UK).

2.1.4. Spread of MG63 cells

Human MG63 osteoblast-like cells were grown to confluence using DMEM with 10% fetal bovine serum (FBS), 100 mg/ml of streptomycin, and 100 units/ml of penicillin under humidified 37℃ and 5% CO_2. Cell monolayers were disrupted and removed using trypsin-EDTA and were seeded on each disc surface at a density of 1.0×10^4 cells/disc. The cells were cultured for 30

minutes and then gently washed with PBS to remove unattached cells. Fixation was carried out with 4.0% formaldehyde at pH 7.4. Samples were dehydrated and coated with gold prior to SEM observation.

For morphometric analysis of the cells, the sizes of 20 randomly-selected cells on the specimens were measured semi-automatically using Paint.NET v3.5 software (dotPDN LLC); cell outlines were drawn manually by controlling the contrast of images obtained under 2,000× magnification, and the surface area of cells was calculated automatically.

Data analysis was performed using the PASW18.0 (SPSS Inc., Chicago, IL, USA) software package. Group comparisons were made with Kruskal-Wallis test, and *p*-values less than 0.05 were accepted as statistically significant.

2.2. Osteoconductivity Tests

2.2.1. Preparation of fixture-shaped specimens

A total of 100 fixture-shaped specimens with the same macro-design (Brånemak type, threaded external hex with a diameter of 4 mm and a length of 7.0 mm) were manufactured by PIM and used for osteoconductivity tests. The properties of the zirconia powder (Tosho, Nanyo, Japan) used in fabricating Y-TZP implants are listed in Table 1. Specimens were divided into four groups (n = 25) as follows:

Group 1: A fixture-shaped specimen (Cetatech, Sacheon, Korea) (Figure 2b, left).

Group 2: A roughened fixture-shaped specimen (Cetatech) (Figure 2b, right).

Group 3: An APP-treated fixture-shaped specimen.

Group 4: APP-treated roughened fixture-shaped specimen.

From each group, histomorphometric analysis was performed with 15 samples and the removal torque tests were carried out using the remaining 10 samples.

2.2.2 Surface analyses

Surface topography of fixture-type specimens were examined using SEM. The average surface roughness (S_a) was obtained by CLSM.

2.2.3. Surgical procedures

Three-month-old New Zealand white rabbits weighing 2.5-3.0 kg (total of 25 animals) were used to assess *in vivo* bone-forming capacity. All animals were housed in stainless steel cages individually with a standard laboratory diet and water *ad libitum*. Animals received general anesthesia by an intramuscular injection of 10 mg/kg zolazepam (Zoletil®, Yuhan Corp., Seoul, Korea) with 10 mg/kg xylazine hydrochloride (Rompun®, Bayer, Frankfurt, Germany). Local anesthesia (lidocaine 2% and epinephrine 1:100,000) was applied at the experimental sites. The hind legs of the animals were shaved before surgery, and the surgeries were performed by an experienced surgeon using aseptic technique. Surgical sites were accessed with 3-cm-long incisions through the skin and fascia. Bone surfaces were exposed using a surgical elevator. Specimens were placed following site preparation using copious saline-cooled 2.0-mm and 3.0-mm twist drills followed by a screw tap. Two fixture-type specimens were placed into each tibial metaphysis. Each group was randomly allocated for implantation in either the left or right hind limb. The plasma-treated specimens were installed within 10 minutes after APP treatment. The fascia and skin were closed in layers with appropriate interrupted single and mattress sutures using resorbable (Vicryl 5.0, Ethicon, Somerville, NJ, USA) or non-resorbable materials (GORETEX Suture CV5, WL Gore & Associates, Flagstaff, AZ, USA). A non-narcotic, non-steroidal analgesic agent with anti-inflammatory and antipyretic activities (flunixinmeglumine, 1.0 mg/kg,

intramuscularly, twice daily for 3 days) was administered for pain control. A broad spectrum antibiotic (cefazolin, 80 mg/kg, intramuscularly, twice daily for 3 days) was administered for infection control. The animals were sedated and euthanized with an overdose of sodium pentobarbital (100 mg/kg) at 4 weeks after the surgical process. Block biopsy specimens were collected from the implant sites, fixed in 10% buffered formalin, and processed for biomechanical and histomorphometric analyses.

Immediately following sacrifice, the bone section was trimmed and cleaned for the removal torque tests. A coupling mount was attached to the implants, and the mount was connected to one arm of a torsional universal testing machine (55MT1-31, Instron, MA, USA) designed to produce a linearly increasing torque. The bone section was coupled to the opposing arm and secured coaxially into a 9/16-inch socket using a light-curing composite. A rotational unscrewing force was applied to the implant, and real time torque values were measured using software (Partner 7.1e, Instron, MA, USA). The peak torque value was recorded in N·cm and represented as the mean ± standard deviation with a significance level of $p < 0.05$.

Samples were rinsed, dehydrated, and embedded in light-curing methacrylate (Technovit 7200 VLC, Kulzer, Wehrheim, Germany). The implants were cut through the mid-axial apico-coronal plane using a macro cutting and grinding

technique (EXAKT 310 CP series, Exakt Apparatebau, Norderstedt, Germany) and were subsequently ground and polished to a final thickness of 30 to 40 μm. The specimens were surface-stained with hematoxylin and eosin.

Histologic analysis of samples was performed throughout the cortical and medullary areas of the bone using a light microscope (Olympus, Tokyo, Japan) with varying magnifications. Histomorphometric analyses were performed by connecting the microscope to a computer. Digital images were captured, and a computer-based image analysis system, Image-Pro Plus (Media Cybernetic, Silver Spring, MD, USA), was used to quantify the findings. The percentages of bone-implant contact (BIC) and bone volume per tissue volume (BV/TV) inside the threads within the cortical resident bone of 15 implants per group were measured. BV/TV was calculated by dividing the area of bone volume (BV) by the total tissue volume (TV) present in the region of interest.[24]

Intra-examiner reliability for histomorphometric evaluation was assessed using the concordance correlation coefficient, which ranges between 0 and 1, with a higher coefficient corresponding to greater reliability. The concordance correlation coefficient for histomorphometric measurements ranged from 0.87 to 0.94, demonstrating high reliability for all assessed parameters.

Statistical analyses of surface roughness and plasma were performed using

ANOVA and *post hoc* tests with Levene's test from PASW Statistics 18 (p=0.05).

Animal selection, management, and surgical protocols were approved and performed under the guidelines of the Institutional Animal Care and Use Committee of Seoul National University.

3. RESULTS

3.1. Cell Spread on APP-treated and Etched Y-TZP Surfaces

The surface area roughness (S_a) was higher in Groups B and D after sandblasting and HF etching (1.01 ± 0.01 ㎛ and 1.00 ± 0.02 ㎛, respectively) compared to that of Groups A and C (0.69 ± 0.08 ㎛ and 0.72 ± 0.03 ㎛, respectively). Both AFM and CLSM observations revealed a uniformly textured microstructure of the Y-TZP discs without topographical changes (Figure 3).

Contact angle analysis indicated that plasma treatment with vaporized DW (Groups C and D) led to contact angles of less than 10 degrees, which is indicative of enhanced hydrophilicity compared with untreated surfaces. The plasma-untreated groups, A and B, showed contact angles of 71.6 ± 6.4° and 71.6 ± 13.6°, respectively. When the surfaces of Groups A and B were plasma-treated without vaporized DW, the contact angles decreased to 34.8 ± 6.9° and 22.6 ± 10.8°, respectively (Figure 4).

Results of XPS analysis are shown in Table 2. The surface of Group A showed atomic percent values of 8.1%, 63.9%, and 28.0% for Zr, C and O, respectively, while the surface analyzed after plasma treatment (Group C)

demonstrated atomic percent values of 17.5%, 29.5%, and 53.0% for Zr, C and O, respectively. Relative to the control surface, the plasma-treated surface exhibited an increase in the Zr, and O atomic percent levels by 9.4% and 25.0%, respectively, and a decrease in C atomic percent levels of 1.5%.

Attached cells observed by SEM are shown in Figure 5. After 30 minutes of incubation, cell size was significantly different depending on the plasma treatment (Table 3). Statistically significant differences were observed between Groups 1 and 2 and Groups 3 and 4; cell size was influenced by the plasma treatment (p=0.000 and 0.000, respectively). The effect of surface roughness between Groups 1 and 3 and Groups 2 and 4 (p=0.045 and 1.000, respectively) was unclear.

3.2. Osteoconductivity Tests

The SEM micrographs demonstrated increased roughness of the surfaces in Groups 2 and 4 (Figure 6b), with the typical grain structure found in Groups 1 and 3 (Figure 6a). The grain structures of both implant surfaces could be easily identified, and the differences between them were obvious under AFM (Figure 6c and 6d). Average surface roughness (S_a) values obtained from CLSM in Groups 1 and 3 (0.54 ± 0.05㎛, 0.54 ± 0.04 ㎛, respectively) were approximately 4 times lower than those of Groups 2 and 4 (1.98 ± 0.14 ㎛, 1.99 ± 0.14 ㎛, respectively).

Healing was uneventful. During the healing period, none of the implants were lost, and all implants were primarily stable and appeared to be clinically osseointegrated. All implants showed peri-implant bone formation (Figure 7). In the cortical compartment, the implants were well surrounded by bone in all tested groups. Under high magnifications (100×), new bone formation and remodeling was also observed. The marrow space within the cancellous bone was filled with vascularized loose connective tissue. The medullary compartments of most implants of Groups 1 and 2 were sparsely covered by isolated bony islands. In contrast, many of the medullary compartments of Groups 3 and 4 were surrounded by more continuous bone, which looked like the trabecular bone extending from the cortical layer.

From the results of histomorphometric analysis (summarized in Table 4) the average BICs for Groups 1, 2, 3, and 4 were 58.26%, 56.93%, 70.88%, and 72.27%, respectively. The average bone volume/total volume (BV/TV) for Groups 1, 2, 3, and 4 were 42.75%, 43.51%, 53.25%, and 55.31%, respectively. The average removal torque values for Groups 1, 2, 3, and 4 were 39.70 N·cm, 59.21 N·cm, 46.75 N·cm, and 60.98 N·cm, respectively. Levene's test showed that the tested samples fulfilled the homogeneity of variance assumption. Statistical analysis indicated that the BIC, BV/TV and removal torque values were significantly different among the groups. For the

BIC ratio, there was a statistically significant difference between Groups 1 and 2 and Groups 3 and 4 according to the *post hoc* test. The removal torque values showed statistically significant differences between Groups 1 and 2 as well as between Groups 1 and 4 (Table 3). Based on statistical analysis, BIC and BV/TV were influenced by plasma treatment (p=0.000 and 0.000, respectively), but not by surface roughness (p=0.658 and 0.990, respectively), nor were they influenced by interaction of the two factors (p=0.940 and 0.623, respectively). The removal torque value was influenced by surface roughness (p=0.000), but not by plasma treatment (p=0.271), nor by the interaction of the two factors (p=0.508).

4. DISCUSSION

Surface topographical analysis indicated no significant differences after APP treatment indicating that the plasma used in this study is able to enhance surface hydrophilicity while minimizing violation of surface topography. In contrast to thermal plasma, non-thermal plasma displays exceptional chemical reactivity, having a relatively mild, non-destructive character, allowing for applications in various fields including surface engineering.[25] Non-thermal plasmas have also been studied in dentistry for various purposes and have been reported to increase the surface wettability of impression material and acrylic resin.[26-28] Recently, argon atmospheric pressure plasma was reported to be effective in enhancing wettability and cell spreading on Ti discs.[29] The surface wettability of a material is directly related to the surface hydrophilic properties. Enhancement of hydrophilic properties has received attention recently, with current findings supporting the biologic implications of hydrophilicity at the initial contact of an implant surface with the host interface.[30] One approach for obtaining hydrophilic and energetic surfaces in Ti implants is to isolate the uncontaminated TiO_2 surface from contact with the atmosphere.[31] Compared with conventional SLA® surfaces (InstitutStraumann AG, Waldenburg, Switzerland) these modified surfaces have been proven to enhance protein adsorption and to promote a

differentiated osteogenic phenotype, although a decrease in cell proliferation was also observed.[31]

The results of XPS showed that surface elemental chemistry was modified by plasma treatment. Combined with the results of contact angle measurements, plasma treatment resulted in a higher degree of exposure of the surface chemical elements mainly at the expense of the removal of adsorbed hydrocarbon contents. The same phenomenon was observed under plasma treatment without vaporized DW. The decreased hydrocarbon content on the surface seemed to significantly affect the surface wettability; plasma treatment with vaporized DW showed increased surface hydrophilicity. An increase in basic hydroxyl OH(b) ions with zirconium and a decrease in the hydrocarbon content seemed to be responsible for the enhanced surface hydrophilicity, similar to what has been seen with osteoblasts on titanium surfaces.[32]

Zirconia implants with smooth surfaces are not well retained. To overcome these challenges, attempts have been made to achieve sufficient roughness for osseointegration.[33, 34] Superhydrophilicity has been obtained by blasting a Y-TZP surface with aluminum oxide particles of 150 ㎛, followed by HF etching.[35] We found that in sandblasted and HF acid-etched surfaces (Groups B and D), the average surface roughness (S_a) was around 1.00 ㎛, which was

only slightly higher than that of a sintered surface. Larger blasting particles have been reported to increase the possibility of introducing microcracks and flaws, which can affect the mechanical properties of Y-TZP.[36] By using a powder injection molding technique, a roughened mold is shown to increase surface roughness (S_a = 1.99 ㎛) up to the level of the SLActive® surface (S_a = 1.75 ㎛), which is currently one of the roughest-surfaced titanium implants,[37] without changing the surface chemistry. However, the optimal roughness of Y-TZP implants for osseointegration is still unclear and should be explored in future studies.

The more hydrophilic surface resulted in significantly higher MG63 cellular attachment, BIC, and BV/TV. The RT value was also higher in Groups 2 and 4, with rough surfaces, although a slight increase in RT value was observed in the plasma treated groups of smooth surface Y-TZP implants. Mechanical testing tends to favor implants with rougher surface profiles due to mechanical interlocking,[38] or the degree of bone maturation (not evaluated in this study) might have influenced the RT value. Serial sectioning at different time intervals should be included in further studies.

Histology showed trabecular bony growth in the fixture-shaped specimens of Groups 3 and 4 located in the medullary area. It is unknown whether this pattern is related to the plasma treatment. Newly formed bone can be seen

around the margin of continuous bone apposition where intimate contact with the experimental fixtures was also observed.

Another point to be addressed is the effective time of the treatment. The increased hydrophilicity obtained by plasma treatment is not long-lasting.[39] The treatment protocol used in the present study did not include a monomer, which is usually incorporated in the plasma coating. Thus, the hydrophilicity began to weaken within the first hour from the onset of treatment and vanished over time. Although determining the effective duration was beyond the scope of this study, special attention was paid to control delays from plasma treatment, minimizing it to ten minutes for all experiments in this study. It is not known how long the hydrophilic effects of APP treatment last; therefore it might be better to install implants as soon as possible after treatment. Since the dimension of the plasma flame has to be compatible with the dental clinic environment, some modification in the equipment should allow for the installation of these implants immediately after plasma treatment. In addition, further assessment of bone maturation should be carried out at multiple intervals post-operatively, in order to elucidate the effects of plasma treatment during the healing phase. Well-designed, hierarchical evaluations are required to establish the clinical applications of this treatment.

5. CONCLUSION

Our results indicated that APP treatment of Y-TZP enhances the spread of MG63 cells *in vitro* as well as osseointegration *in vivo* in rabbits. Surface micro-topographies did not appear to change substantially with treatment but the hydrophilic property changed considerably. New trabecular bony growth was observed, although it is unclear whether this resulted directly from the plasma treatment.

REFERENCES

1. Pjetursson BE, Thoma D, Jung R, Zwahlen M, Zembic A. A systematic review of the survival and complication rates of implant-supported fixed dental prostheses (FDPs) after a mean observation period of at least 5 years. Clin Oral Implants Res 2012;23 Suppl 6:22-38.
2. Jung RE, Pjetursson BE, Glauser R, et al. A systematic review of the 5-year survival and complication rates of implant-supported single crowns. Clin Oral Implants Res 2008;19(2):119-30.
3. Weingart D, Steinemann S, Schilli W, et al. Titanium deposition in regional lymph nodes after insertion of titanium screw implants in maxillofacial region. Int J Oral Maxillofac Surg 1994;23(6 Pt 2):450-2.
4. Bianco PD, Ducheyne P, Cuckler JM. Local accumulation of titanium released from a titanium implant in the absence of wear. J Biomed Mater Res 1996;31(2):227-34.
5. Prithviraj DR, Deeksha S, Regish KM, Anoop N. A systematic review of zirconia as an implant material. Indian J Dent Res 2012;23(5):643-9.
6. Sailer I, Zembic A, Jung RE, et al. Randomized controlled clinical trial of customized zirconia and titanium implant abutments for canine and posterior single-tooth implant reconstructions: preliminary results at 1 year of function. Clin Oral Implants Res 2009;20(3):219-25.
7. Buser D, Broggini N, Wieland M, et al. Enhanced bone apposition to a chemically modified SLA titanium surface. J Dent Res 2004;83(7):529-33.
8. Davies JE. Mechanisms of endosseous integration. Int J Prosthodont

1998;11(5):391-401.

9. Le Guehennec L, Lopez-Heredia MA, Enkel B, et al. Osteoblastic cell behaviour on different titanium implant surfaces. Acta Biomater 2008;4(3):535-43.

10. Anselme K, Bigerelle M. Statistical demonstration of the relative effect of surface chemistry and roughness on human osteoblast short-term adhesion. J Mater Sci Mater Med 2006;17(5):471-9.

11. Ball M, Grant DM, Lo WJ, Scotchford CA. The effect of different surface morphology and roughness on osteoblast-like cells. J Biomed Mater Res A 2008;86(3):637-47.

12. Ito H, Sasaki H, Saito K, et al. Response of osteoblast-like cells to zirconia with different surface topography. Dent Mater J 2013;32(1):122-9.

13. Hoffmann O, Angelov N, Zafiropoulos GG, Andreana S. Osseointegration of zirconia implants with different surface characteristics: an evaluation in rabbits. Int J Oral Maxillofac Implants 2012;27(2):352-8.

14. Park YS, Chung SH, Shon WJ. Peri-implant bone formation and surface characteristics of rough surface zirconia implants manufactured by powder injection molding technique in rabbit tibiae. Clin Oral Implants Res 2013;24(5):586-91.

15. Song JH. The injection-monding of fine and ultra fine zirconia powders. Ceramics International 1995;21:325-33.

16. Wennerberg A, Albrektsson T. Effects of titanium surface topography on bone integration: a systematic review. Clin Oral Implants Res 2009;20 Suppl 4:172-84.

17. Rupp F, Scheideler L, Eichler M, Geis-Gerstorfer J. Wetting behavior of dental implants. Int J Oral Maxillofac Implants 2011;26(6):1256-66.

18. Kim MH, Lee SY, Kim MJ, et al. Effect of biomimetic deposition on anodized titanium surfaces. J Dent Res 2011;90(6):711-6.

19. Tan F, Naciri M, Al-Rubeai M. Osteoconductivity and growth factor production by MG63 osteoblastic cells on bioglass-coated orthopedic implants. Biotechnol Bioeng 2011;108(2):454-64.
20. Lang NP, Salvi GE, Huynh-Ba G, et al. Early osseointegration to hydrophilic and hydrophobic implant surfaces in humans. Clin Oral Implants Res 2011;22(4):349-56.
21. Huang HM, Hsieh SC, Teng NC, et al. Biological surface modification of titanium surfaces using glow discharge plasma. Med Biol Eng Comput 2011;49(6):701-6.
22. Yousfi M, Merbahi N, Pathak A, Eichwald O. Low-temperature plasmas at atmospheric pressure: toward new pharmaceutical treatments in medicine. Fundam Clin Pharmacol 2013.
23. Cho BH, Han, G. J., Oh, K. H., Chung, S. N. & Chun, B. H. The effect of plasma polymer coating using atmospheric-pressure glow discharge on the shear bond strength of composite resin to ceramic. Journal of Materials Science 2011;46(8):2275-763.
24. Gahlert M, Roehling S, Sprecher CM, et al. In vivo performance of zirconia and titanium implants: a histomorphometric study in mini pig maxillae. Clin Oral Implants Res 2012;23(3):281-6.
25. Loh JH. Plasma surface modification in biomedical applications. Med Device Technol 1999;10(1):24-30.
26. Cokeliler D, Erkut S, Zemek J, Biederman H, Mutlu M. Modification of glass fibers to improve reinforcement: a plasma polymerization technique. Dent Mater 2007;23(3):335-42.
27. Puleo DA, Kissling RA, Sheu MS. A technique to immobilize bioactive proteins, including bone morphogenetic protein-4 (BMP-4), on titanium alloy. Biomaterials 2002;23(9):2079-87.
28. Hayakawa T, Yoshinari M, Nemoto K. Characterization and protein-adsorption behavior of deposited organic thin film onto titanium by plasma polymerization with hexamethyldisiloxane. Biomaterials

2004;25(1):119-27.

29. Duske K, Koban I, Kindel E, et al. Atmospheric plasma enhances wettability and cell spreading on dental implant metals. J Clin Periodontol 2012;39(4):400-7.

30. Sela MN, Badihi L, Rosen G, Steinberg D, Kohavi D. Adsorption of human plasma proteins to modified titanium surfaces. Clin Oral Implants Res 2007;18(5):630-8.

31. Zhao G, Schwartz Z, Wieland M, et al. High surface energy enhances cell response to titanium substrate microstructure. J Biomed Mater Res A 2005;74(1):49-58.

32. Feng B, Weng J, Yang BC, Qu SX, Zhang XD. Characterization of surface oxide films on titanium and adhesion of osteoblast. Biomaterials 2003;24(25):4663-70.

33. Aboushelib M, Salem N, Abotaleb A, Abd El Moniem N. Influence of surface nano-roughness on osseointegration of zirconia implants in rabbit femur heads using selective infiltration etching technique. J Oral Implantol 2011.

34. Wang G, Liu X, Zreiqat H, Ding C. Enhanced effects of nano-scale topography on the bioactivity and osteoblast behaviors of micron rough ZrO2 coatings. Colloids Surf B Biointerfaces 2011;86(2):267-74.

35. Noro A, Kaneko M, Murata I, Yoshinari M. Influence of surface topography and surface physicochemistry on wettability of zirconia (tetragonal zirconia polycrystal). J Biomed Mater Res B Appl Biomater 2013;101(2):355-63.

36. Atsu SS, Kilicarslan MA, Kucukesmen HC, Aka PS. Effect of zirconium-oxide ceramic surface treatments on the bond strength to adhesive resin. J Prosthet Dent 2006;95(6):430-6.

37. Wennerberg A, Albrektsson T. On implant surfaces: a review of current knowledge and opinions. Int J Oral Maxillofac Implants

2010;25(1):63-74.

38. Gotfredsen K, Berglundh T, Lindhe J. Anchorage of titanium implants with different surface characteristics: an experimental study in rabbits. Clin Implant Dent Relat Res 2000;2(3):120-8.

39. Guastaldi FP, Yoo D, Marin C, et al. Plasma treatment maintains surface energy of the implant surface and enhances osseointegration. Int J Biomater 2013;2013:354125.

FIGURE LEGENDS

Figure 1. (a) Schematic diagram of the chair-side non-thermal atmospheric plasma equipment, a modification from the design by Cho et al.[22] Plasma treatment was performed at a distance of 5 mm for 60 seconds. (b) Plasma treatment of the disc and (c) implant samples.

Figure 2. Experimental samples of (a) the disc-shaped (Groups A-D) and (b) the fixture-type (Groups 1-4) specimens. The implant fixture on the left shows Groups 1 and 3 manufactured with an untreated mold, while the roughened surfaces of Groups 2 and 4 are shown on the right.

Figure 3. Representative AFM (a and b) and CLSM (c and d) images of disc specimens (Groups A-D). Microscopic images showed uniform distribution of surface irregularities of each surface. The average surface roughness (S_a) of sandblasted/HF-etched surfaces (Groups B and D shown in Figure 3d) were 1.01 ㎛ and 1.00 ㎛, respectively, which was higher than those in untreated surfaces (Groups A and C shown in Fig. 3c, S_a = 0.69 ㎛ and 0.72 ㎛, respectively).

Figure 4. Contact angle measurements. The contact angle after plasma treatment without DW (b) significantly decreased compared with the untreated surface (a), but not as much as the plasma with vaporized DW (c).

Figure 5. Representative SEM images (2000×) of MG63 cells on each disc surface after 30 minutes of incubation. (a) Group A; (b) Group B; (c) Group C; and (d) Group D.

Figure 6. SEM and AFM images of the fixture-type specimens. Groups 1 and 3, which were manufactured with an untreated mold (a and c), showed average surface roughness (S_a) of 0.54 ㎛ and 0.54 ㎛, respectively. (b and d) Roughened inner molds (Groups 2 and 4) showed average surface roughnesses (S_a) of 1.98 ㎛ and 1.99 ㎛, respectively.

Figure 7. Undecalcified section stained with hematoxylin and eosin. Direct contact between the bone and the implant surface is shown. The fixture-type specimens of Groups 3 and 4 show trabecular bone extending to the medullary region. (a, b) Group 1; (c,d) Group 2; (e,f) Group 3 and (g,h) Group 4.

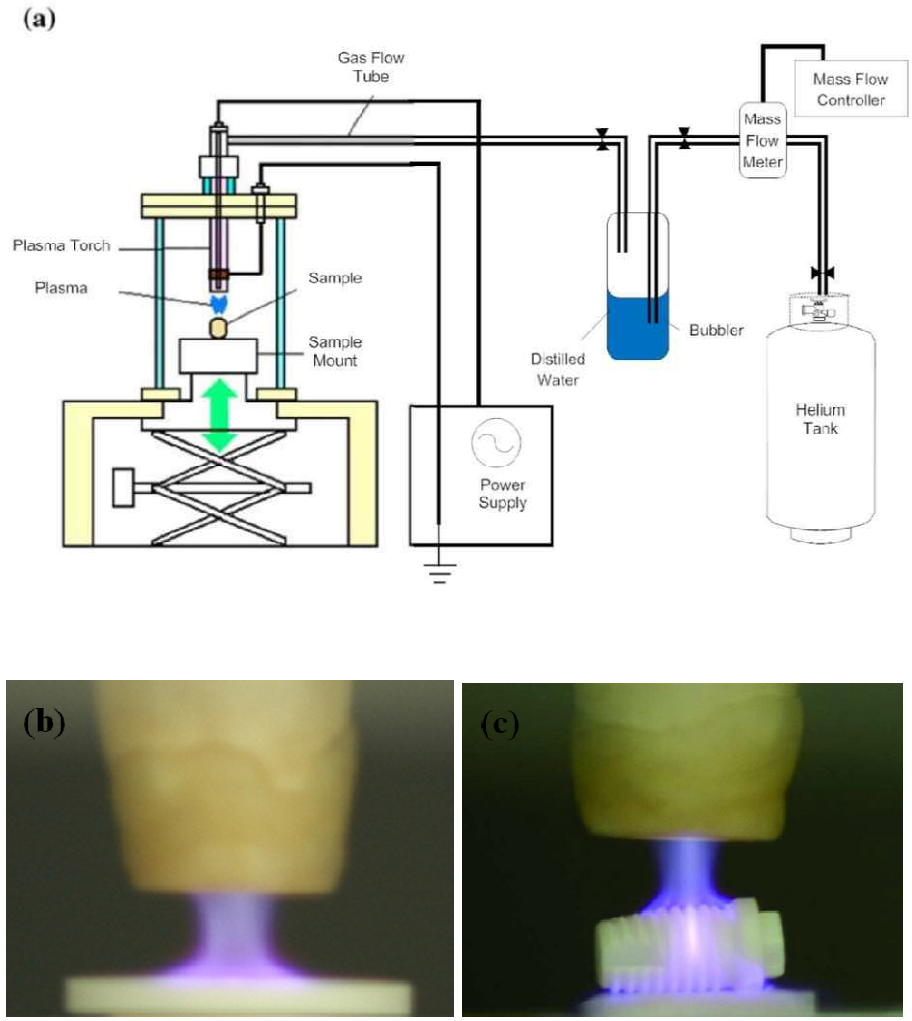

Figure 1. (a) Schematic diagram of the chair-side non-thermal atmospheric plasma equipment, a modification from the design by Cho et al.[22] Plasma treatment was performed at a distance of 5 mm for 60 seconds. (b) Plasma treatment of the disc and (c) implant samples.

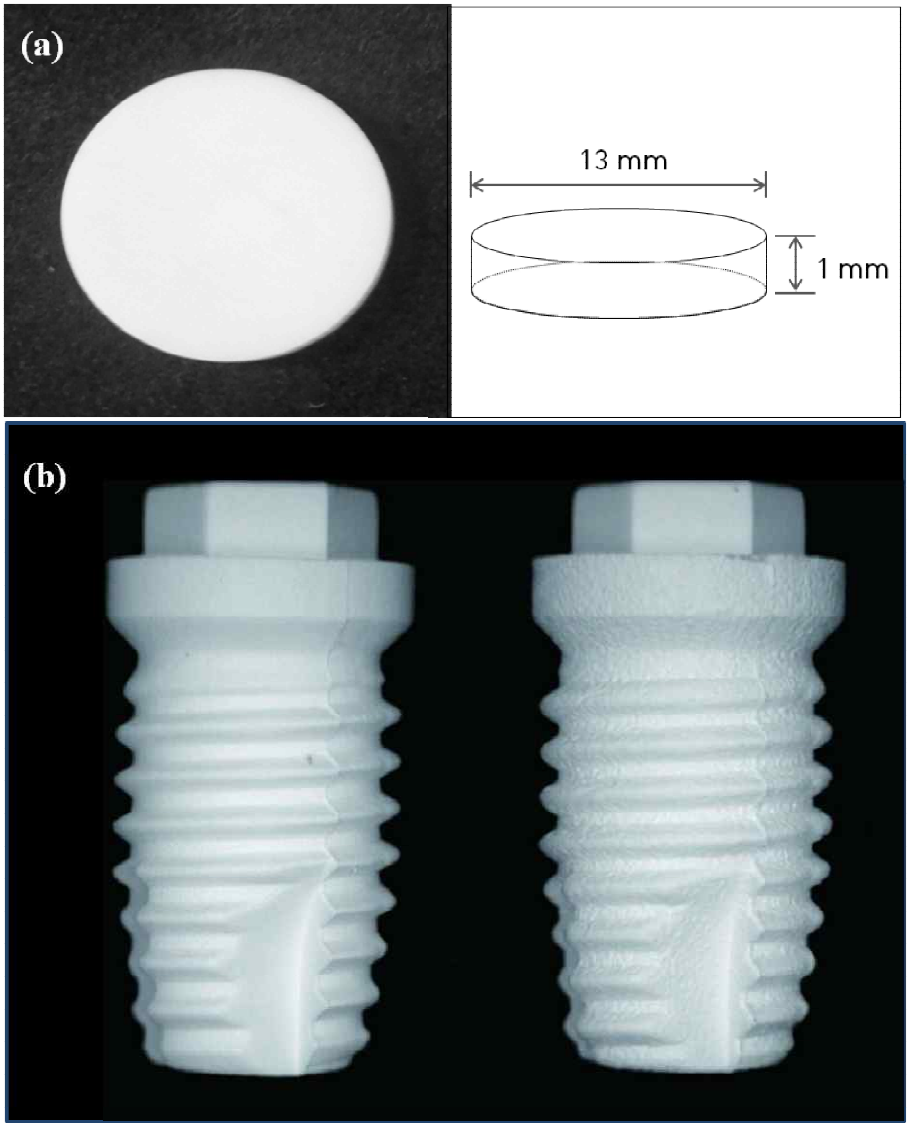

Figure 2. Experimental samples of (a) the disc-shaped (Groups A-D) and (b) the fixture-type (Groups 1-4) specimens. The implant fixture on the left shows Groups 1 and 3 manufactured with an untreated mold, while the roughened surfaces of Groups 2 and 4 are shown on the right.

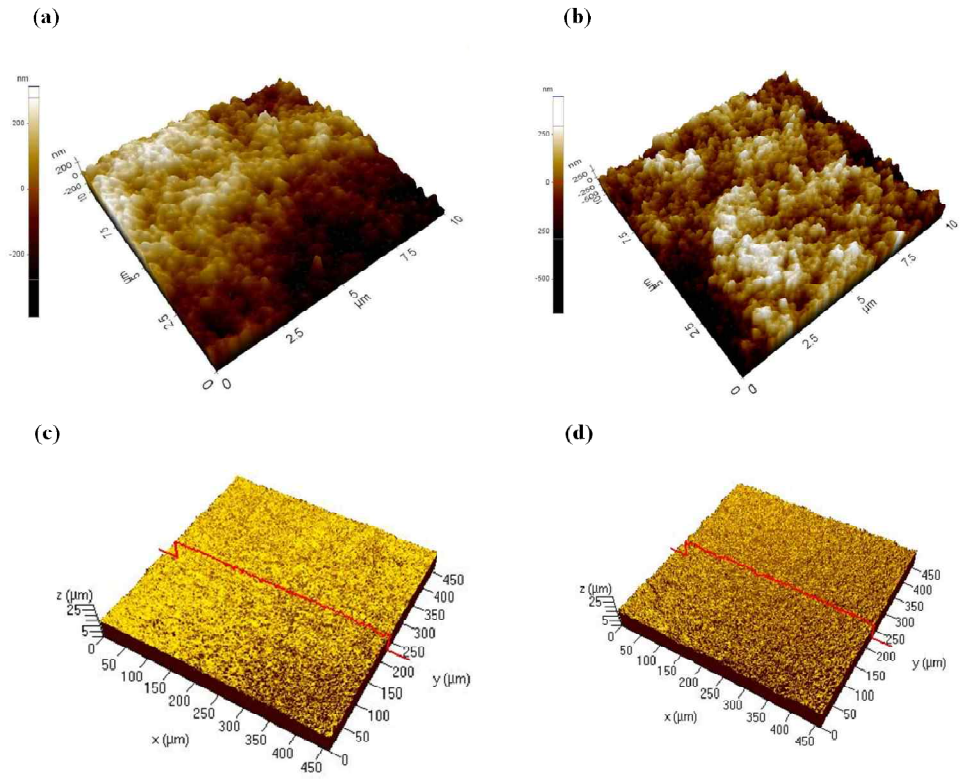

Figure 3. Representative AFM (a and b) and CLSM (c and d) images of disc specimens (Groups A-D). Microscopic images showed uniform distribution of surface irregularities of each surface. The average surface roughness (S_a) of sandblasted/HF-etched surfaces (Groups B and D shown in Figure 3d) were 1.01 ㎛ and 1.00 ㎛, respectively, which was higher than those in untreated surfaces (Groups A and C shown in Fig. 3c, S_a = 0.69 ㎛ and 0.72 ㎛, respectively).

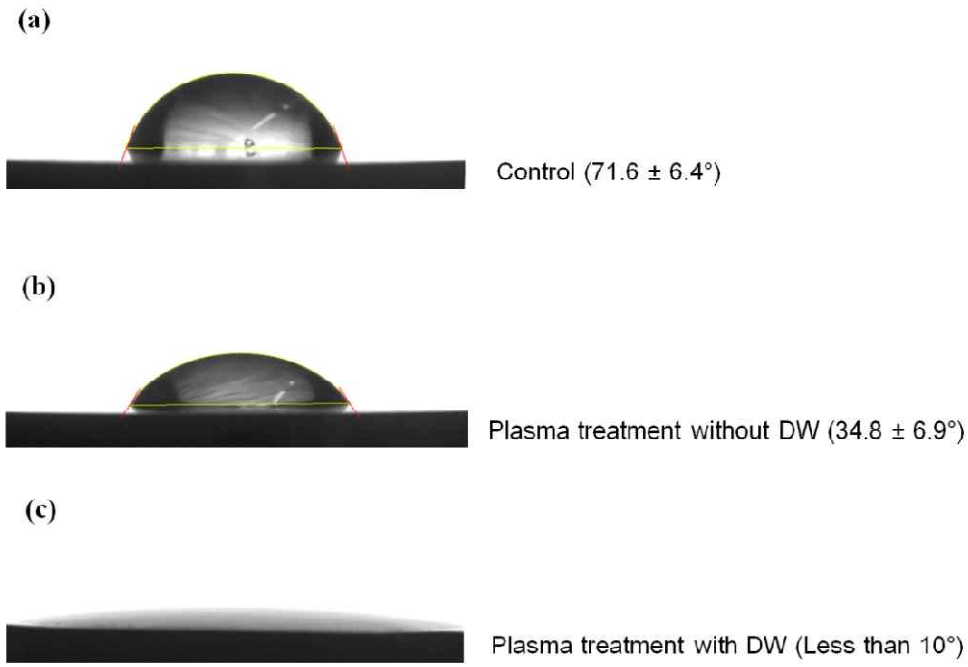

Figure 4. Contact angle measurements. The contact angle after plasma treatment without DW (b) significantly decreased compared with the untreated surface (a), but not as much as the plasma with vaporized DW (c).

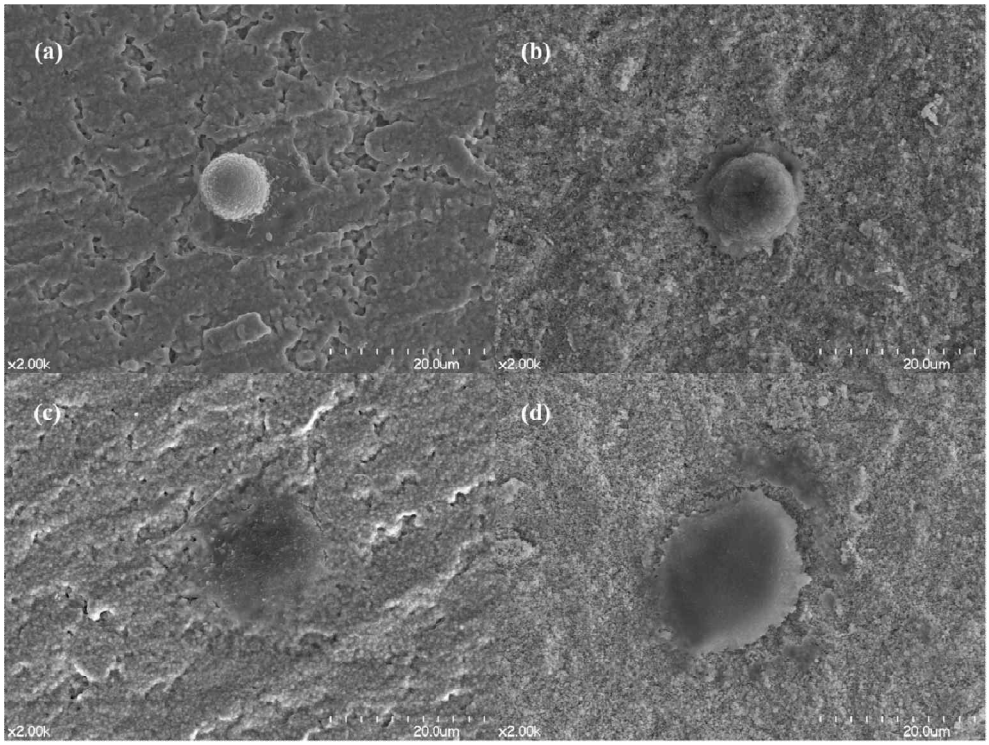

Figure 5. Representative SEM images (2000×) of MG63 cells on each disc surface after 30 minutes of incubation. (a) Group A; (b) Group B; (c) Group C; and (d) Group D.

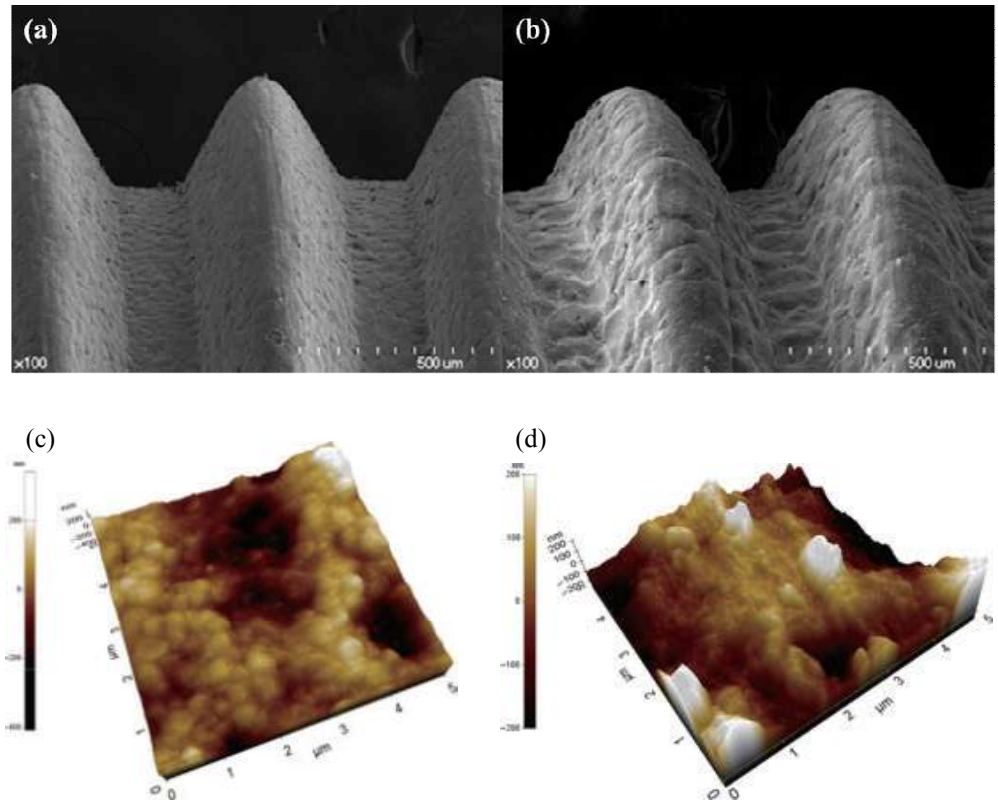

Figure 6. SEM and AFM images of the fixture-type specimens. Groups 1 and 3, which were manufactured with an untreated mold (a and c), showed average surface roughness (S_a) of 0.54 ㎛ and 0.54 ㎛, respectively. (b and d) Roughened inner molds (Groups 2 and 4) showed average surface roughnesses (S_a) of 1.98 ㎛ and 1.99 ㎛, respectively.

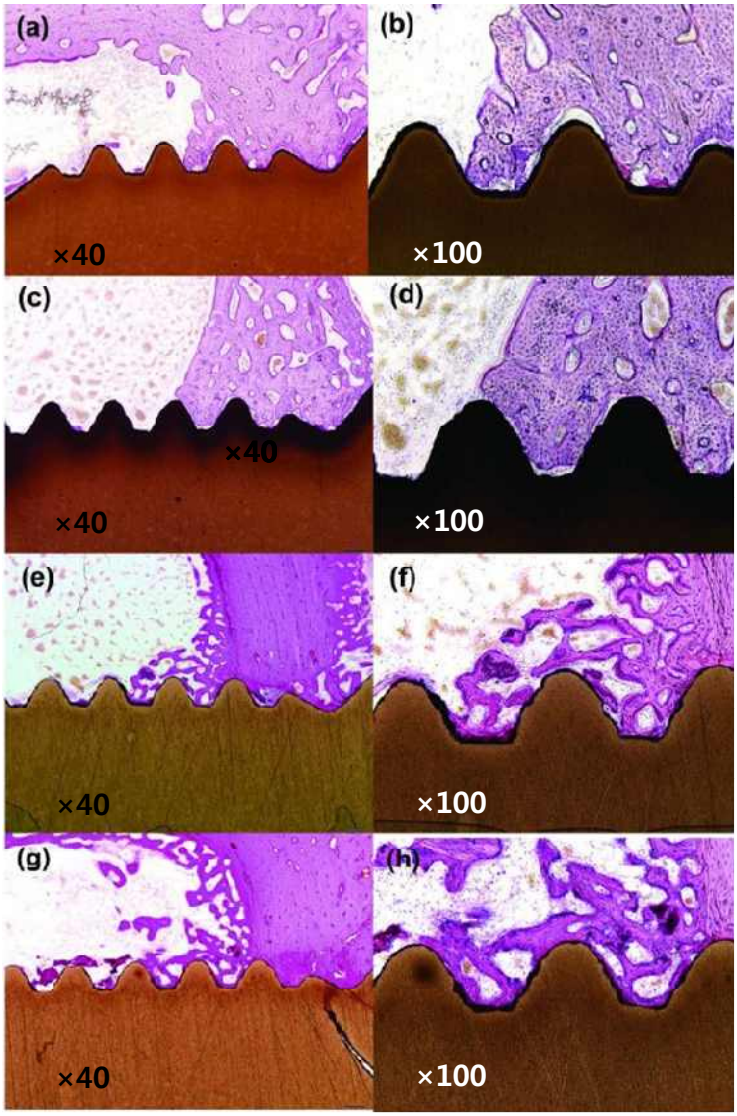

Figure 7. Undecalcified section stained with hematoxylin and eosin. Direct contact between the bone and the implant surface is shown. The fixture-type specimens of Groups 3 and 4 show trabecular bone extending to the medullary region. (a, b) Group 1; (c,d) Group 2; (e,f) Group 3 and (g,h) Group 4.

Table 1. Properties of the zirconia powder used in the study.

Powder Characteristics	
ZrO_2	95.62 (wt. %)
Y_2O_3	5.18 (wt. %)
Al_2O_3	0.253 (wt. %)
SiO_2	max. 0.002 (wt. %)
Fe_2O_3	max. 0.002 (wt. %)
Na_2O	0.006 (wt. %)
Specific Surface Area	6.8 (m^2/g)
Crystallite Size	360 (Å)

Table 2. XPS analysis of the surfaces. (a) Decreased hydrocarbon contents with (b) increased basic hydroxyl group contents after the plasma treatment

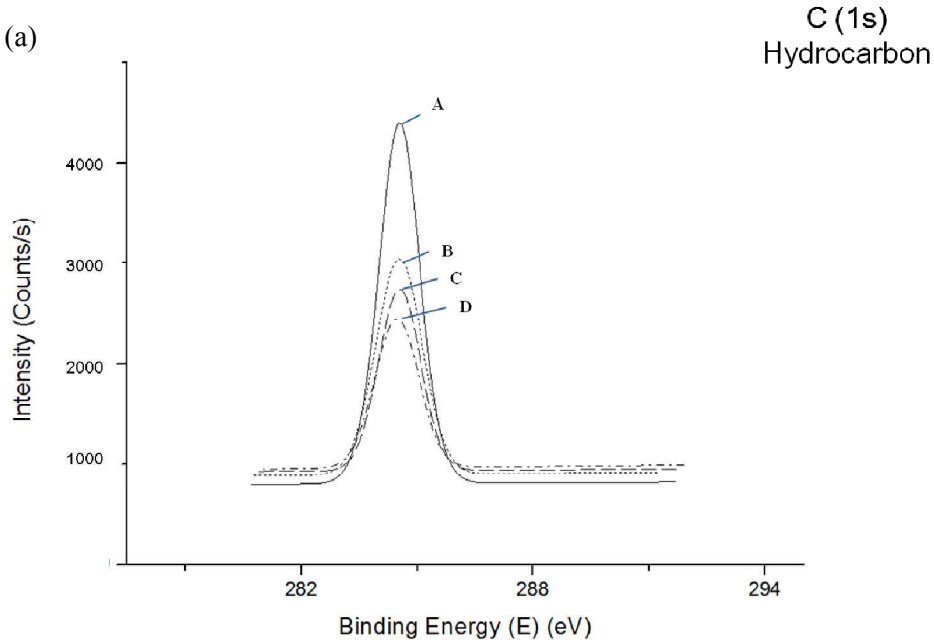

Label	Peak BE (eV)	Height Counts	FWHM (eV)	Area	At. %
A (control)	284.53	3602.29	1.29	4831.91	47.58
B (rough)	284.52	2149.26	1.43	3267.01	33.22
C (plasma)	284.53	1818.06	1.29	2482.8	24.62
D (rough/plasma)	284.47	1495.72	1.36	2145.08	21.41

(b)

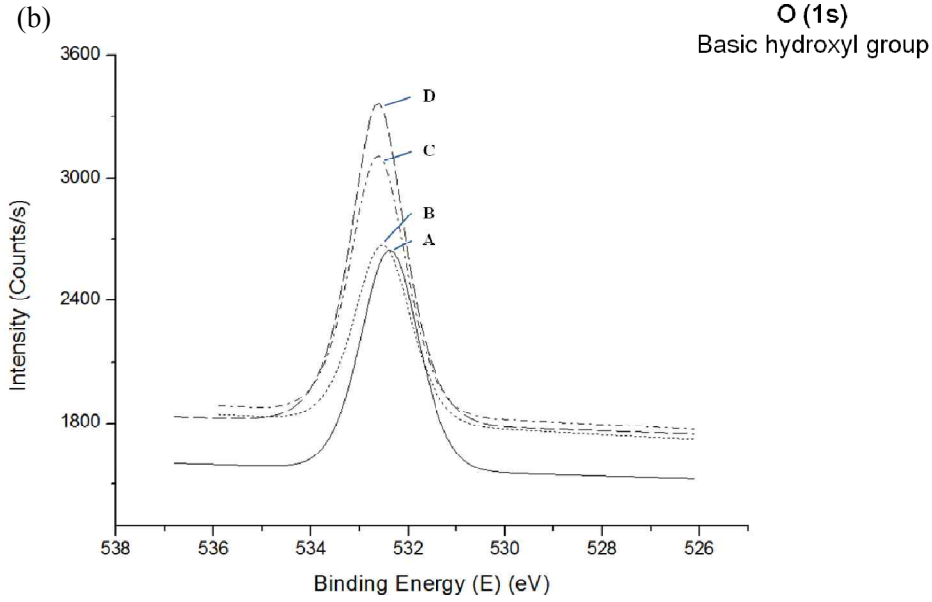

Label	Peak BE (eV)	Height Counts	FWHM (eV)	Area	At. %
A (control)	532.39	1075.59	1.45	1632.1	5.29
B (rough)	532.53	873.57	1.41	1299.64	4.35
C (plasma)	532.63	1567.14	1.35	2341.01	7.63
D (rough/plasma)	532.62	1265.03	1.38	1863.65	6.12

Table 3. Measurements of MG63 cell size after 30 minutes of incubation

Disc Specimens	Morphometric analysis (n=20) (μm^2, mean ± standard deviation)
Group A (Control)	225.67 ± 97.89^{a}
Group B (Sandblast/HF etched)	140.55 ± 51.13^{a}
Group C (Plasma Group A)	755.50 ± 362.98^{b}
Group D (Plasma Group B)	838.68 ± 109.51^{c}

* The same superscripts indicate lack of statistically significant differences between groups.

Table 4. Results of bone–implant contact (BIC) ratio values (percent, mean ± standard deviation [SD]), bone volume (BV/TV, bone volume/total volume) values and removal torque (RT) values for the tested implants

Implant Group	Histomorphometric analysis		RT (N·cm)
	BIC (n=15)	BV/TV (n=15)	(n=10)
	(%, mean ± standard deviation)		
Group 1 (Control)	58.26 ± 10.09[a]	42.75 ± 9.68[a]	39.70 ± 11.69[a]
Group 2 (Rough)	56.93 ± 12.95[a]	43.51 ± 7.23[a]	59.21 ± 12.35[b]
Group 3 (Plasma Group 1)	70.87 ± 9.11[b]	53.25 ± 6.88[b]	46.75 ± 13.15[ab]
Group 4 (Plasma Group 2)	72.27 ± 10.31[b]	55.31 ± 7.48[b]	60.98 ± 12.70[b]

* The same superscripts indicate lack of statistically significant differences between groups after Scheffe's *post hoc* tests

국문 초록

지르코니아의 표면 거칠기와 상압 플라즈마 처리가 골양 세포 및 골 형성에 미치는 영향에 관한 연구

서울대학교 대학원 치의과학과 치과보존학 전공
(지도교수 손 원 준)
정 신 혜

연구목적: 본 연구에서는 거칠기를 부여한 지르코니아(Y-TZP) 표면에서 상압 플라즈마 처리가 골양 세포의 확산과 골 형성에 미치는 영향을 *in vitro*와 *in vivo*에서 평가하고자 한다.

재료 및 방법: 원반 형태(Ø 13 × 1 mm)의 시편은 샌드 블라스팅 처리 후 불산 부식을 통해 거칠기를 부여하였고, 거칠기와 플라즈마 처리 유무에 따라 네 개의 그룹으로 나누었다. 표면은 X 선 회절 분석과 접촉각 측정을 통해 분석하였고, 공초점 레이저 현미경 하에서 표면 조도를 측정하였다. 또한, MG 63 세포 부착 30분 후 세포 확산 정도를 전자 현미경으로 관찰하였다.

생체 내 실험은 임플란트 형태(Ø 4 × 7 mm)의 시편을 이용하였다. 시편은 거친 몰드를 이용하여 분말사출성형법으로 표면 거칠기를 부여하였으며 거칠기와 플라즈마 처리 유무에 따라 네 개의 그룹으로 나누었다. 총 25 마리의 토끼 경골에 매식 4주 후 removal

torque test (RTQ)와 조직형태학적 분석을 시행하였다. 이원분산분석을 통하여 통계학적 유의성을 분석하였다 (p=0.05).

결 과: 상압 플라즈마 처리 후 지르코니아(Y-TZP) 표면은 강한 친수성을 나타내었다. 원반 형태의 시편에서 플라즈마 처리 과정에 의한 표면의 형태변화는 보이지 않았으며 30분 후 세포 확산이 유의성 있게 증가하였다. 임플란트 형태 시편에서는 플라즈마 처리 후 유의성 있게 높은 bone-to-implant contact (BIC) ratio와 bone volume ratio (BV/TV)가 관찰되었다.

결 론: 상압 플라즈마 처리에 의해 지르코니아 표면은 강한 친수성을 나타내었으며 초기 MG63 세포의 확산 및 임플란트 골 유착이 증가하였다.

주요어: 지르코니아(Y-TZP), 상압 플라즈마, 표면거칠기, 골유착, 친수성

학 번: 2011-30673